Reaction of Hydroxyl Radical with Acetone. 2. Products and Reaction Mechanism

Ranajit K. Talukdar, Tomasz Gierczak,† David C. McCabe,‡ and A. R. Ravishankara*,‡

Aeronomy Laboratory, National Oceanic and Atmospheric Administration, 325 Broadway, Boulder, Colorado 80305, and Cooperative Institute for Research in Environmental Sciences, University of Colorado, Boulder, Colorado 80309

Received: October 24, 2002; In Final Form: February 19, 2003

The products of the reaction of OH with acetone (OH + $CH_3C(O)CH_3$ → products) were investigated using a discharge flow tube coupled to a chemical ionization mass spectrometer. It was shown that the yield of acetic acid from the reaction was less than 1% between 237 and 353 K. The yield of acetonyl radical was measured to be (96 ± 11)%, independent of temperature, between 242 and 350 K. The rate coefficients for the reaction were measured with this system to be the same as those reported in part 1 (*J. Phys. Chem. A* **2003**, *107*, 5014). The rate coefficients for the removal of OH ($v = 1$) by acetone and acetone-d_6 were shown to be (2.67 ± 0.15) × 10^{-11} and (3.45 ± 0.24) × 10^{-11} cm^3 $molecule^{-1}$ s^{-1}, respectively, at 295 K. It was shown that the enthalpy of reaction for the formation of an OH−acetone adduct is more than −8 kcal mol^{-1} (i.e., the adduct is bound by at most 8 kcal mol^{-1}) at 203 K. On the basis of these observations and those from part 1, we deduce that the reaction of OH with acetone occurs through a hydrogen-bonded complex that gives almost exclusively $CH_3C(O)CH_2$ and H_2O. The atmospheric implications of our findings are discussed.

1. Introduction

In part 1 of this paper[1] we have reported our results on the kinetics of the reaction of OH with acetone, reaction 1:

$$OH + CH_3C(O)CH_3 \rightarrow \text{products} \quad (1)$$

Here, we discuss our measurements of the product yields in reaction 1 and our investigations of the mechanism of this reaction. The possible exothermic channels for the reaction of OH with acetone include:

$$OH + CH_3C(O)CH_3 \rightarrow CH_3C(O)CH_2 + H_2O \qquad \Delta_rH^0 = -21.0 \text{ kcal mol}^{-1} \quad (1a)$$

$$OH + CH_3C(O)CH_3 \rightarrow CH_3C(O)OH + CH_3 \qquad \Delta_rH^0 = -25.7 \text{ kcal mol}^{-1} \quad (1b)$$

Recently Wollenhaupt and Crowley[2] reported the yield of CH_3, i.e., channel 1b, to be 0.5 and 0.3 at 297 and 233 K, respectively. Vasvári et al.[3] measured the yield of $CH_3C(O)CH_2$ (acetonyl radical) from channel 1a to be 0.5 and concluded that the yield of acetic acid (channel 1b) was 0.5, in agreement with Wollenhaupt and Crowley.[2] While our work was in progress, Tyndall et al.[4] and Vandenberk et al.[5] reported upper limits of <10% and <5%, respectively, for the yield of acetic acid in reaction 1 at 298 K. They concluded that reaction 1 predominantly (yield > 90%) proceeds via channel 1a.

In addition to the experimental studies, several groups have investigated reaction 1 theoretically.[3,5−7] Vasvári et al.[3] explored the pathways for H atom abstraction and for OH addition to the carbonyl-C, which could lead to production of acetic acid, via ab initio quantum chemical calculations. In contrast to their experimental findings, Vasvári et al. calculated a substantial barrier for OH addition to the carbonyl-C. They also examined a pathway where the H atom in OH approaches the carbonyl oxygen atom to form a hydrogen-bonded six-membered ring similar to that suggested for the reaction of OH with HNO_3.[8] A previous report from our group has suggested a similar mechanism.[9] Such a reaction pathway should yield $CH_3C(O)CH_2$ and H_2O. Vandenberk et al.[5] also theoretically examined the OH addition followed by CH_3-elimination channel (1b), a direct H-abstraction channel (1a), and an indirect H-abstraction channel via a six-membered hydrogen-bonded OH-acetone complex (1a). They found the barrier for OH addition to the carbonyl-C to be (6.0 ± 0.5) kcal mol^{-1}, at least 2.5 kcal mol^{-1} higher than that for the direct H-abstraction channel. They suggested that the indirect H-abstraction channel, including tunneling, could explain the low-temperature behavior of k_1. Aloisio and Francisco[10] also calculated that a H-bonded six-membered ring OH−acetone complex is stable with respect to reactants by 5.3 kcal mol^{-1} (i.e., $\Delta_rH^0 = -5.3$ kcal mol^{-1}) at 300 K.

In this paper we present our results on the products and mechanism of reaction 1. First, we identify and quantify acetonyl and $CD_3C(O)CD_2$ (acetonyl-d_5) radicals, respectively, as the major, if not the sole, products of reactions 1 and 2.

$$OH + CD_3C(O)CD_3 \rightarrow \text{Products} \quad (2)$$

Second, we present experimental evidence to show that the acetic acid yield in reaction 1 is negligible. Third, we place an upper bound on the bond strength of a possible OH−acetone adduct. Finally, we present a model for reaction 1 that accounts for all of our experimental observations and reproduces the measured values of k_1 as a function of temperature.

* Corresponding author. Address: NOAA/ERL, R/AL2, 325 Broadway, Boulder, CO 80305. E-mail: ravi@al.noaa.gov.

† Permanent address: Department of Chemistry, Warsaw University, ul. Zwirki i Wigury 101, 02-089 Warsaw, Poland.

‡ Also associated with the Department of Chemistry and Biochemistry, University of Colorado, Boulder, CO 80309.

10.1021/jp0273023 CCC: $25.00
Published on Web 06/04/2003

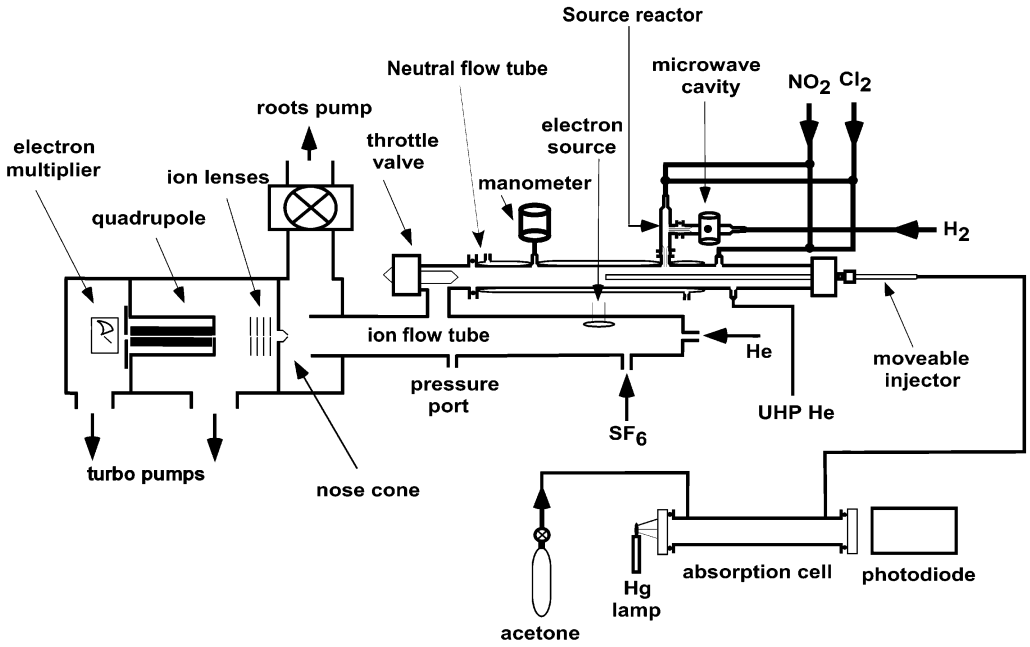

Figure 1. Experimental apparatus used to measure the rate coefficients and products of reaction 1. The reaction of OH with acetone was carried out in the neutral flow tube and the concentrations of reactants and products were measured using the ion flow tube (where chemical ionization occurred) and the quadrupole mass spectrometer.

For atmospheric purposes, it is important to quantify the products of reaction 1. If this reaction formed acetic acid, the acid could lead to new particle formation and loss of acetone degradation products via rain out/precipitation before the products react to form species that generate HO_x in the atmosphere.

2. Apparatus

During this work we used pulsed laser photolysis−pulsed laser induced fluorescence (PP-PLIF) to examine the possible formation of an OH−acetone adduct, to investigate some possible isotopic exchange reactions, and to measure the rate coefficients for the removal of vibrationally excited OH ($X^2\Pi$, $v = 1$) by acetone and acetone-d_6. This apparatus has been described in part 1.[1] We also used a discharge flow tube coupled to a chemical-ionization mass spectrometer (DF−CIMS) to determine the rate coefficient of reaction 1 and the products of reactions 1 and 2.

A schematic of the chemical ionization mass spectrometer-flow tube apparatus is shown in Figure 1. It consisted of a flow tube reactor (hereafter referred to as the neutral flow tube, NFT) where OH reacted with acetone. A separate reactor, called the source reactor (SR), was attached to the NFT for radical generation. The NFT was coupled to an ion flow tube where reagent ions were generated and selectively reacted with the molecules of interest. A quadrupole mass spectrometer detected and quantified the ions exiting the ion flow tube. Details of the ion flow tube, reagent ion generation, and the measurements of reaction rate coefficients of neutral radical-molecule reactions using DF−CIMS have been described previously.[11−13]

2.1. Neutral Flow Tube (NFT) and Radical Generation. The neutral flow tube reactor was a 150-cm jacketed Pyrex tube with an internal diameter of 2.54 cm. The effluents of the neutral flow tube passed through a Pyrex valve into the ion flow tube, ∼50 cm downstream of the ionization source. The Pyrex valve controlled the gas flow rate out of the NFT and therefore its pressure. Pressure in the NFT (1.1−3.2 Torr) was significantly greater than that in the ion flow tube (∼0.5 Torr). The excess reactant gas (in bath gas) was added to the NFT through a 120-cm, 0.64-cm diameter moveable Pyrex injector. The position of the injector in the NFT could be varied along a 50-cm long reaction zone. The radical reactant (in bath gas) was introduced 16 cm upstream of the temperature-controlled region. Flow rates of UHP He between 600 and 1500 STP cm^3 min^{-1} in the NFT produced linear flow velocities between 600 and 3000 cm s^{-1}. The pressure at the middle of the reaction zone was measured by a capacitance manometer. The reactor was cooled or heated by passing a temperature-controlled fluid through the jacket. A chromel−alumel thermocouple, inserted through the injector, measured the temperature of the carrier gas in the reaction zone; the variation in the temperature of the carrier gas in this zone was ≤1 K. To minimize the effects of heterogeneous reactions, the outside of the injector, the inside of the NFT, and the Pyrex valve were coated with halocarbon wax.

In the present study, the OH and OD radicals and Cl atoms were produced in the source reactor (SR) attached to the NFT. A microwave discharge produced H atoms. A constriction (15 mm long × 2 mm i.d.) between the microwave discharge region and the SR minimized back diffusion into the discharge. The SR (20 cm long × 1.27 cm o.d.) was coated with halocarbon wax to reduce radical loss on its walls. This reactor was always maintained at room temperature.

The H(D) atoms were generated in a low-power (∼30 W) microwave discharge through a 1% mixture of $H_2(D_2)$ in UHP He. The hydrogen atoms (or D atoms) reacted in the SR either with Cl_2 to give Cl (used for calibration of the acetonyl radical signal) or with NO_2 to give OH(OD) radicals:

$$H(D) + Cl_2 \rightarrow Cl + HCl(DCl) \quad (3)$$

$$H(D) + NO_2 \rightarrow OH(OD) + NO \quad (4)$$

These reactions are fast [$k_{3(H)} = (2.52 \pm 0.18) \times 10^{-11}$ cm^3 molecule^{-1} s^{-1} (ref 14) and $k_{3(D)} = 1.4 \times 10^{-11}$ cm^3 molecule^{-1} s^{-1} (ref 15); $k_{4(H\&D)} = \sim 1.3 \times 10^{-10}$ cm^3 molecule^{-1} s^{-1} (refs 16 and 17)] and were driven to completion (>99%) in the SR {[NO_2] ≈ (2−5) × 10^{12} and [Cl_2] ≈ (1−4) × 10^{13} molecule cm^{-3} in the SR, reaction time (10−20 ms)}.

TABLE 1: Ion−Molecule Reaction Schemes Employed in Detecting Various Radicals and Molecules in This Study

species to be detected	reaction scheme	ions detected (*m*/*e*)	sensitivity[d]
OH	$OH + SF_6^- \rightarrow OH^- + SF_6$	OH^- (17)	2.5×10^8
OH[a]	$OH + CS_2^- \rightarrow HS^- + OCS$	HS^- (33)	3×10^8
NO_2	$NO_2 + SF_6^- \rightarrow NO_2^- + SF_6$	NO_2^- (46)	1×10^9
NO_2[a]	$NO_2 + CS_2^- \rightarrow NO_2^- + CS_2$	NO_2^- (46)	2×10^8
H(D)	$H(D) + CS_2^- \rightarrow HS^-(DS^-) + CS$	$HS^-(DS^-)$/33 (34)	3×10^8
Cl	$Cl + SF_6^- \rightarrow Cl^- + SF_6$	Cl^- (35)	1×10^{10}
CH_3COOH	$CH_3COOH + SF_6^- \rightarrow CH_3COO^- + SF_5 + HF \rightarrow (CH_3COO\bullet HF)^- + SF_5$	$(CH_3COO\bullet HF)^-$ (79)	3×10^8 [b,c]
$CH_3C(O)CH_2$	$CH_3C(O)CH_2 + CS_2^- \rightarrow (CH_3C(O)CH_2\bullet CS_2)^-$	$(CH_3C(O)CH_2\bullet CS_2)^-$ (133)	5×10^8
$CD_3C(O)CD_2$	$CD_3C(O)CD_2 + CS_2^- \rightarrow (CD_3C(O)CD_2\bullet CS_2)^-$	$(CD_3C(O)CD_2\bullet CS_2)^-$ (138)	5×10^8

[a] Used when acetone was present. [b] In the presence of 3×10^{15} molecule cm^{-3} of acetone in the NFT. [c] The detection sensitivity for acetic acid in the absence of acetone in the NFT was 6×10^8 molecule cm^{-3}. [d] Sensitivities are in units of molecule cm^{-3} in the NFT for a $S/N = 1$ (see text).

2.2. Ion Detection Schemes. The reagent ions for chemical ionization, SF_6^- and CS_2^-, were produced by attachment of thermalized electrons to SF_6 and CS_2, respectively. A small fraction of the reagent ions reacted with the reactant and product molecules of interest from the NFT to generate the ions that were detected by the quadrupole mass spectrometer. The concentrations of the detected ions were proportional to the products of the concentrations of the neutral molecules and the rate coefficients for their reactions with the reagent ions.

The ion−molecule reactions employed to detect various reactants and products in our experiments are listed in Table 1.

2.2.1. OH and NO_2 Detection. The OH radicals from the NFT reacted with SF_6^- in the ion flow tube to generate OH^-.

$$OH + SF_6^- \rightarrow OH^- + SF_6 \qquad (5)$$

We used reaction 5 in some experiments. However, in the presence of a large quantity of acetone, $(1-10) \times 10^{13}$ molecule cm^{-3} (in the ion flow tube), OH^- reacted with acetone in the ion flow tube. Therefore, a sufficient concentration of CS_2 ($\sim 3 \times 10^{13}$ molecule cm^{-3}) was added to the ion flow tube reactor downstream of the ion source to completely (>99%) convert OH^- to HS^-.[13]

$$OH^- + CS_2 \rightarrow HS^- + OCS \qquad (6)$$

Thus, the OH radical was detected as HS^- at mass 33. OD was detected in a similar way as DS^- at mass 34. (HS^- and DS^- did not measurably react with acetone.)

NO_2 was converted to NO_2^- via reaction with SF_6^-.

$$NO_2 + SF_6^- \rightarrow NO_2^- + SF_6 \qquad (7)$$

The product ion signals (OH^-, HS^-, and NO_2^-) were proportional to the concentrations of OH and NO_2 at the exit of the neutral flow tube. The CIMS signals for OH and NO_2 were calibrated to the concentration of these radicals in the NFT as described previously.[12]

2.2.2. Detection of Acetic Acid. SF_6^- was again used as the reagent ion. Acetic acid reacts rapidly with SF_6^- via F^- transfer to give $(CH_3COO\bullet HF)^-$, which was detected at mass 79:

$$CH_3C(O)OH + SF_6^- \rightarrow (CH_3COO\bullet HF)^- + SF_5 \qquad m/e = 79 \text{ amu} \quad (8a)$$

$$\rightarrow CH_3COO^- + SF_5 + HF \qquad m/e = 59 \text{ amu} \quad (8b)$$

The CH_3COO^- ($m/e = 59$) produced by channel 8b was not used in quantifying $CH_3C(O)OH$ because of a interfering signal at *m*/*e* of 59 attributed to $(HF)_2 \cdot F^-$. In addition to the mass peaks at 59 and 79, acetic acid also produced a peak at mass 99, which could be attributed to $HF \cdot (CH_3COO \cdot HF)^-$, formed by clustering of an $(CH_3COO \cdot HF)^-$ ion with HF, which was unavoidably present in the ion flow tube.

$$(CH_3COO\bullet HF)^- + HF \rightarrow [CH_3COO\bullet (HF)_2]^- \qquad m/e = 99 \text{ amu} \quad (9)$$

Acetic acid was quantified by monitoring only mass 79. In acetic acid yield experiments, the initial concentration of OH was determined via reaction 5 before addition of acetone.

2.2.3. Detection of Acetonyl Radical, $CH_3C(O)CH_2$. CS_2^- was used as the reagent ion. The signal at $m/e = 133$ was observed in the mass spectrum upon generation of acetonyl radical via reaction 1 in the neutral flow tube. The peak at $m/e = 133$ is assigned to the cluster of acetonyl radical with CS_2^- on the basis of the dependence of its count rate on the OH radical concentration: it depleted linearly upon decreasing NO_2 flow in the hydroxyl radical source, and it disappeared upon switching off the microwave discharge (no H atom generation). The detection of acetonyl radical was confirmed by producing it via the reaction of chlorine atom with acetone

$$Cl + CH_3C(O)CH_3 \rightarrow CH_3C(O)CH_2 + HCl \qquad (10)$$

and observing the same ion at $m/e = 133$. The addition of only acetone to the ion flow tube in the presence of CS_2^- did not lead to signal at $m/e = 133$. The exact structure of the $(CH_3C(O)CH_2\bullet CS_2)^-$ cluster and the ion−molecule reaction scheme leading to its formation were not investigated. We also used the reaction of Cl with $CD_3C(O)CD_3$ to produce $CD_3C(O)CD_2$, which was detected as an adduct with CS_2^- at mass 138. There was no mass peak observed at $m/e = 138$ in the absence of $CD_3C(O)CD_3$. This observation further confirmed the detection of the acetonyl radical. We found that HCl, produced in reaction 10 and from the subsequent chain reaction of acetonyl radical with Cl_2 present in the NFT (see below), reduced the observed $(CH_3C(O)CH_2\bullet CS_2)^-$ signal at $m/e = 133$.

2.3. Materials. UHP He (99.9999%) with flow rates between 600 and 1500 STP cm^3 min^{-1} was used as bath gas in the NFT. A mixture of 0.5% NO_2 in UHP He was prepared manometrically and stored in a 12-L darkened glass bulb. Dilute mixtures of H_2, D_2, and Cl_2 were either prepared on-line or taken from manometrically prepared stock mixtures. The concentration of Cl_2 in the mixture was checked by UV absorption at 330 nm ($\sigma_{Cl_2} = 2.55 \times 10^{-19}$ cm^2 molecule^{-1}) using a D_2 lamp/diode array spectrometer combination.

Acetone (acetone-d_6) vapor was diluted with He and the concentration of acetone (acetone-d_6) in this mixture was measured in a 10-cm absorption cell at 298 K, using a Hg lamp at 184.9 nm (see part 1: $\sigma_{acetone}^{184.9nm} = 2.98 \times 10^{-18}$ cm^2

molecule^{-1}; $\sigma^{184.9nm}_{acetone-d_6} = 3.91 \times 10^{-18}$ cm^2 molecule^{-1}). This mixture was added to the gases flowing through the NFT. The concentration of acetone (acetone-d_6) in the NFT was calculated from the measured concentration of acetone (acetone-d_6) in the absorption cell, the flow rates of the gases entering the absorption cell and the NFT, and the pressures and temperatures of the absorption cell and the NFT.

All flow rates were measured with electronic mass flow meters, which were calibrated by flowing the gas in use into a known volume and by measuring the rate of pressure change in that volume. Pressures were measured using calibrated capacitance manometers.

3. Experiments and Results

We present here the determinations of the rate coefficients of reaction 1 in the temperature range 238−353 K and the yields of $CH_3C(O)CH_2$ and $CH_3C(O)OH$ in reaction 1 between 237 and 353 K using DF−CIMS. We also present the determinations of the upper limit for the bond enthalpy of the OH−acetone adduct, the rate coefficient for the removal of OH ($v = 1$) by acetone, and the rate coefficient for the exchange of ^{18}OH to ^{16}OH by reaction with acetone. For ease of presentation, we describe the relevant experimental details along with the obtained results.

3.1. OH + Acetone Rate Coefficient, k_1. The rate coefficients for the reactions of OH with acetone, k_1, and acetone-d_6, k_2, were measured under pseudo-first-order conditions in [OH] with a large excess of acetone (3×10^{13} to 3×10^{14} molecule cm^{-3}), which was introduced to the NFT via the moveable injector. Such a procedure is described elsewhere.[11] The variation of OH concentration, as measured by the HS^- ion signal, with the injector distance from the detector was used to derive the pseudo-first-order rate coefficient for the loss of OH, k_i', where $i = 1$ and 2 for acetone and acetone-d_6, respectively. This rate coefficient is equal to (k_i[acetone/acetone-d_6] + k_d) and it was measured at various concentrations of acetone or acetone-d_6. From the variation of k_1' or k_2' with acetone or acetone-d_6 concentrations, the rate coefficient k_1 or k_2 was determined between 238 and 353 K. The obtained rate coefficients are discussed in part 1 along with those measured using PP-PLIF.

3.2. Determination of the Products of Reaction 1. To quantify the yields of $CH_3C(O)OH$ and $CH_3C(O)CH_2$, it was essential to know the concentrations of reactants lost and products formed. We calibrated the response of the CIMS to the reactant, OH, and the products, acetic acid and acetonyl ($CH_3C(O)CH_2$) radical.

3.2.1. Calibration of Reactant and Product Signals. Calibration of OH Signal. A mixture of H_2 in He ([H_2] ≈ 5×10^{12} molecule cm^{-3}) was passed through a microwave discharge and flowed into the NFT. Various small measured concentrations of NO_2 were introduced through the moveable inlet (injector) to completely convert NO_2 to OH. Hydrogen atom concentration was in great excess over that of NO_2. The OH signal was recorded as a function of [NO_2] (Figure 2). The concentration of OH was taken to be the concentration of added NO_2. The measured OH signal varied linearly with [OH] for concentrations up to 1×10^{12} cm^{-3}. The sensitivity for OH detection was 2.5×10^8 cm^{-3} in the neutral flow tube for a signal-to-noise ratio of unity for 10 scans (10 ms residence time on the peak for each scan with a mass resolution of 0.1 amu). The signal-to-noise ratio is defined as the ratio of the count rate (Hz) at the specific mass peak in the presence of OH to the standard deviation of the count rate (Hz) from 10 scans at the same mass peak in the absence of OH. In some experiments, OH radical was generated using reaction 4 in the source reactor and was calibrated in the same way; the signals were the same. This established that the loss of OH before the NFT was not significant.

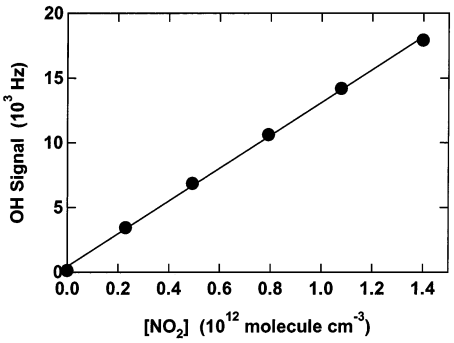

Figure 2. A plot of signal from OH produced by adding known concentrations of NO_2 to an excess of H atoms versus concentration of added NO_2. Such plots were used to calibrate the OH signal.

Calibration of Acetic Acid Signal. We used two acetic acid standards: a manometrically prepared mixture of acetic acid and helium in a Pyrex bulb and a commercial permeation tube. We took into account the fraction of the acetic acid present as dimers ($K_{eq} = 6.8 \times 10^{-17}$ cm^3 molecule^{-1} at 298 K)[18] in the manometrically prepared mixture. The permeation tube consisted of a thin-wall Teflon tube that contained liquid acetic acid. It was placed in a Teflon assembly (8 cm long × 1.5 cm i.d.), which was placed in an oven maintained at 333 K. According to the manufacturer, acetic acid permeated through the Teflon wall with an emission rate of 658 ng min^{-1} at 333 K. Helium carrier gas at ∼600 Torr was flowed through the assembly with a typical flow rate of ∼80 STP cm^3 min^{-1}. The acetic acid/He mixture entered the NFT with the main stream of the carrier gas. The concentration of acetic acid in the NFT was calculated from the emission rate, total flow rate, and pressure in the NFT; typically, the acetic acid concentration was $\sim 2.5 \times 10^{10}$ molecule cm^{-3} but ranged from 2×10^{10} to 7×10^{11} molecule cm^{-3}. Since its concentration in the neutral flow tube was low, acetic acid existed only as the monomer (>99.995% monomer). The CIMS signal of acetic acid was plotted against its calculated concentration and the two sources agreed to within 5% after accounting for the dimers that existed in the Pyrex bulb. The plot was linear between 1×10^{10} to 1×10^{12} molecule cm^{-3} and yielded a small positive intercept consistent with the measured background signal in the absence of acetic acid. Detection sensitivity for acetic acid was determined to be 3×10^8 cm^{-3} in the presence of $(2-3) \times 10^{15}$ molecule cm^{-3} of acetone (same as in actual experiments) for a signal-to-noise ratio of unity for 10 scans (defined in a manner similar to that for OH).

3.2.2. Yields of Products. Yield of Acetonyl ($CH_3C(O)CH_2$)/($CD_3C(O)CD_2$) radical (Channel 1a). Known concentrations of acetonyl radical were produced by the reaction of Cl atom with acetone (reaction 10), which is known to almost exclusively (>97%) give this radical.[19] Small concentrations of H atom were produced in the microwave discharge and titrated in the SR with NO_2 or Cl_2 to produce OH or Cl in back-to-back experiments with [H] kept constant. Thus, the initial concentrations of hydroxyl radical ($[OH]_0$) and chlorine atom ($[Cl]_0$) in the NFT were the same. The yield of $CH_3C(O)CH_2$ radical in reaction 1 relative to that in reaction 10 was determined by monitoring mass 133, $(CH_3C(O)CH_2 \bullet CS_2)^-$ cluster, first with Cl_2 flowing through the SR to produce Cl atom (with NO_2 bypassing the

TABLE 2: Measured Yield of Acetonyl Radical, Φ_a, in Reaction 1, Relative to that from Reaction 10, and the Experimental Conditions under which Φ_a was Determined[a]

T (K)	P_{NFT} (Torr)	$[OH]_{SR}$ (10^{12} molecule cm^{-3})	$[OH]_{NFT}$ (10^{11} molecule cm^{-3})	$[acetone]_{NFT}$ (10^{15} molecule cm^{-3})	Φa[b]	$\langle \Phi a \rangle \pm 2\sigma$[c]
			OH + Acetone			
242	1.5	4.7	3.7	3.1	0.89	0.87 ± 0.06
					0.85	
270	1.4	3.7	2.7	2.05	0.98	0.97 ± 0.05
					0.97	
					0.98	
					0.93	
296	3.1	4.3	4.9	1.8	0.93	1.05 ± 0.20
					0.98	
					0.92	
					1.19	
					1.16	
					1.05	
					1.09	
296	1.1	4.8	2.9	0.8	1.02	0.99 ± 0.10
					0.95	
296	2.0	4.8	4.2	1.45	1.05	
296	1.6	5.3	4.7	1.85	0.85	0.87 ± 0.06
					0.89	
296	1.6	3.7	3.1	1.85	0.91	0.92 ± 0.02
					0.93	
296	1.1	2.6	1.65	0.8	0.92	0.95 ± 0.07
					0.97	
351	1.6	2.4	3.1	1.9	0.83	0.92 ± 0.11
					0.92	
					1.00	
					0.96	
					0.91	
			OH + Acetone-d_6			
296	2.1	5.2	4.3	4.2	1.09	
296	2.1	5.8	5.2	3.2	1.01	
350	2.0	5.3	3.5	2.5	1.18	
			OD + Acetone-d_6			
296	2.0	6.1	4.0	2.5	1.16	
			OD + Acetone			
296	2.0	7.0	5.8	2.5	1.28	

[a] NFT, neutral flow tube; SR, source reactor. [b] Φ_a = Ratio of the normalized signals of acetonyl radical produced in the reactions of OH with acetone and of Cl with acetone. [c] Average of ratios Φ_a at each temperature.

SR into the NFT) and then with NO_2 flowing through the SR to make OH (with Cl_2 bypassing the SR into the NFT). To ensure that the sensitivity for the detection of $CH_3C(O)CH_2$ radical did not change between the two back-to-back experiments using OH and Cl, flow rates of all the reactants and buffer gases were kept constant. Mass spectral scans showing the mass peaks at $m/e = 133$ for 296 and 242 K are plotted in Figure 3. The small background at $m/e = 133$ with the microwave discharge off was subtracted from the signals from $CH_3C(O)CH_2$ radical. The ratios of the signals from reaction 1 to that from reaction 10 are listed in Table 2. Our measured yield of $CH_3C(O)CH_2$ radical from the OH reaction is slightly smaller than that from the Cl reaction. This smaller than unity relative yield could be attributed to the higher wall loss and/or faster self-reaction of OH compared to Cl in the source reactor rather than a truly different yield of $CH_3C(O)CH_2$ from reactions 1 and 10. The measured yields were the same, within the experimental uncertainty, when the pressure (1−3 Torr), temperature (242−351 K), or the concentrations of OH (and hence Cl) were varied. The average value is 0.99 ± 0.11 (2σ). Assuming the previously reported yield of acetonyl radical from reaction 10 of 0.97,[19] we obtain an average yield in reaction 1 of 0.96 ± 0.11. Thus we conservatively assign a lower limit of >0.85 for the yield of acetonyl radical in reaction 1. We obtained similar ratios (within the measurement uncertainty) of the OH to Cl reaction yield in the case of reaction 2 (see Table 2). Even substitution of OH by OD produced acetonyl radical with a yield of unity.

Uncertainties in the measured yield of acetonyl radical in reaction 1 come from the uncertainty[19] in the yield of acetonyl radical in reaction 10 and the possible inequality between $[OH]_0$ and $[Cl]_0$. Differences in the wall loss rates of the reactant OH or Cl, and the loss rates of the product acetonyl radical under different conditions, would also contribute to the uncertainty. Radical−radical reactions are unimportant under these conditions. Nielsen et al.[19] determined the yield of $CH_3C(O)CH_2$ radical in reaction 10 to be >97%; small amounts of CH_3Cl and $CH_3C(O)Cl$ were also detected. We carried out a numerical simulation[20] of the reactions that can occur in the SR and thus contribute to an error in the measured value of the acetonyl radical yield. Loss of Cl atom due to recombination and wall loss is small. It was calculated that the concentration of OH dropped by ∼8% (mainly due to its self-reaction), when $[H]_0$ was 5×10^{12} cm^{-3} in the source reactor. The yield of acetonyl radicals was not strongly affected by any small OH loss because [OH] in the SR was kept lower than 5×10^{12} radical cm^{-3} in the majority of the experiments. Thus, the lower limit of 0.85 appears to be valid.

In the main neutral flow tube, the acetonyl radical should react with Cl_2, producing Cl atom, which in turn would react rapidly with acetone to regenerate acetonyl radical. The regeneration of acetonyl radical and the production of HCl by

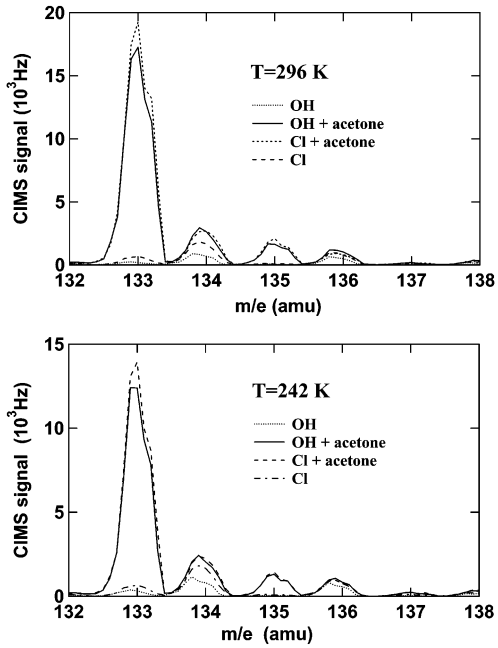

Figure 3. Mass spectra of the effluents of the neutral flow tube with different reagents added to the flow tube at 296 K (upper panel) and 242 K (lower panel). Mass scans with only OH, OH and acetone, Cl and acetone, and only Cl added to the neutral flow tube are shown. For $T = 296$ K (upper panel), $[OH]_0 = [Cl]_0 = 3.1 \times 10^{11}$ radical cm^{-3} and [acetone] $= 1.85 \times 10^{15}$ molecule cm^{-3}. For $T = 242$ K (lower panel), $[OH]_0 = [Cl]_0 = 3.7 \times 10^{11}$ radical cm^{-3} and [acetone] $= 3.1 \times 10^{15}$ molecule cm^{-3}. The production of acetonyl radicals from the reaction of OH with acetone and Cl with acetone at two different temperatures is clearly visible.

reaction 10 was the same in both the OH and the Cl reactions, because essentially the same concentration of Cl_2 was present in both cases. The regeneration reduced the loss of acetonyl radical in the NFT, but the HCl it produced reduced the observed acetonyl signal (equally for both the OH and Cl reactions). The concentrations of HCl produced in this regeneration could be higher than $[Cl]_0$: [HCl] in the neutral flow tube could reach 6×10^{12} molecule cm^{-3} when $[Cl]_0$ was 2×10^{12} molecule cm^{-3}. Thus, the observed acetonyl radical signal would be decreased, although the radical concentration would not decrease in the NFT. However, we maintained $[OH]_0$ and $[Cl]_0$ at $<6 \times 10^{11}$ cm^{-3}, thereby limiting the amount of HCl formed to less than 2×10^{12} molecule cm^{-3}, which avoided any significant interference in the quantification of acetonyl radical.

Yield of Acetic Acid, Φ_b. The yield of acetic acid was determined by monitoring mass 79 ($CH_3COOH{\cdot}F^-$) by scanning the mass range between 74 and 82 amu in the following sequence: (1) with only OH present, (2) with acetone present but no OH, (3) with the OH source on and acetone present, (4) with OH and acetone present and a known concentration of acetic acid added to the neutral flow tube. A sequence of scans for steps 1−4 is shown in Figure 4. The concentrations of added acetic acid (in step 4) for the data in this figure were roughly equal to that expected from reaction 1 if the yield were ∼2% (in step 3). The initial concentration of OH, $[OH]_0$, in the NFT was held constant through the sequence (except in step 2) and was quantified before and after each experiment, as described before. The upper limit for the concentration of acetic acid produced by reaction 1 was determined by subtracting the signal at $m/e = 79$ obtained in step 2 from the signal obtained in step 3 and then comparing this signal level to the additional signal at the same mass present in step 4. The signal at $m/e = 79$ with just OH and its precursors present, i.e., step 1, was very small.

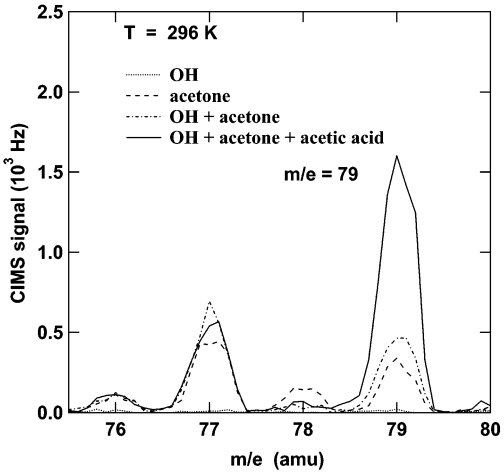

Figure 4. Mass spectra of the effluents of the neutral flow tube (at 296 K) with the following reagents added to the flow tube: only OH (1.2×10^{12} molecule cm^{-3}), dotted line; only acetone (2.6×10^{15} molecule cm^{-3}), dashed line; OH and acetone, dashed−dotted line; OH, acetone and acetic acid (2.6×10^{10} molecule cm^{-3}), solid line.

The upper limit to the yield of acetic acid from reaction 1 was then obtained by comparing the amount of acetic acid present in step 3 to $[OH]_0$. The signal level in step 4 was not affected by the presence of OH. Results for the yields obtained using this method, between 237 and 353 K, are listed in Table 3, along with the experimental conditions used for the measurements. Because the signal we saw in step 3 could have come from sources other than reaction 1, we quote these as upper limits.

The loss of OH in the source reactor due to self-reaction could be important at high concentrations of OH, because its concentration in the SR is almost an order of magnitude higher than that in the NFT. Therefore, $[OH]_0$ (in the NFT) was maintained in the range $(4-36) \times 10^{10}$ molecule cm^{-3}. To ensure minimal loss of OH in the NFT, the concentration of acetone was kept high enough ($2-3 \times 10^{15}$ molecule cm^{-3}) to react away all OH within 10 cm (flow velocities 600−800 cm s^{-1}) after mixing.

Acetic acid yield in the reaction of OD with acetone

$$OD + CH_3C(O)CH_3 \rightarrow CH_3C(O)CH_2 + HOD \quad (11a)$$

$$\rightarrow CH_3C(O)OD + CH_3 \quad (11b)$$

at 296 K was determined to be <0.001, which was essentially the same as that for reaction 1 (Table 3). Although the mass peak would be expected at $m/e = 80$ if $CH_3C(O)OD$ is formed, because of H−D exchange in the ion flow tube, we detected the peak at $m/e = 79$. We could not measure the yield of acetic acid-d_3 in the reaction of OH with acetone-d_6 because the signal expected at mass peak 82 had a large background. These experiments clearly show that the yield of acetic acid is negligible (<1%) in reactions 1 and 11 under the conditions of all of our experiments.

The small variations in the upper limits for the yields shown in Table 3 were due to the signal that could be attributed to acetic acid, which was always near our detection limit. If a very small concentration of acetic acid were produced in reaction 1, it could have been lost heterogeneously on the flow tube wall and thus appear to not have been formed. However, small amounts of acetic acid that were intentionally added were not lost. Also, variation in $[OH]_0$ by a factor of ∼9 (and hence the concentration of possible acetic acid produced) did not change the observed yield of acetic acid. The concentration of acetic

TABLE 3: Measured Yield of Acetic Acid, Φ_b, in Reaction 1, and the Experimental Conditions under which Φ_b was Determined

T (K)	P (Torr)	[acetone] (10^{15} molecule cm^{-3})	[acetic acid][a] (10^{11} molecule cm^{-3})	$[OH]_0$ (10^{11} molecule cm^{-3})	[acetic acid][b] (10^{9} molecule cm^{-3})	Φ_b[c]
			OH + Acetone			
237	3.1	0.8	4.55	6.3	2.8	0.0045
237	3.1	0.8	4.64	23.0	6.9	0.003
238	1.1	1.1	0.88	4.4	2.6	0.006
296	3.2	1.3	6.69	22.5	26	0.0117
296	3.1	2.3	4.05	36.0	22	0.006
296	3.1	2.6	3.54	9.4	1.9	0.002
296	3.1	2.5	3.75	10.0	5	0.005
296	3.1	2.6	0.26[d]	12.0	0.72	0.0006
296	3.1	2.6	0.26[d]	12.0	0.84	0.0007
296	3.0	2.8	0.26[d]	23.0	1.6	0.0007
333	3.2	2.6	0.23[d]	13.6	0.95	0.0007
333	3.2	2.6	0.23[d]	12.5	0.62	0.0005
353	2.9	2.1	0.21[d]	9.1	1.8	0.002
353	3.2	2.3	0.21[d]	9.2	0.46	0.0005
353	3.2	2.3	0.22[d]	10.8	1.1	0.001
			OD + Acetone			
296	3.0	2.8	0.26[d]	23.0	1.6	0.0007

[a] Added to the flow tube for signal calibration. [b] Upper limit of acetic acid produced in reaction 1. [c] Φ_b was calculated from the signal obtained from reaction 1, the signal from the small known amount of acetic acid added to the NFT, and $[OH]_0$. [d] The permeation tube was used as the source of the known concentration of $CH_3C(O)OH$. In other experiments, a stock mixture of acetic acid in He was used (see text).

acid added to this system was changed by a factor of ~35 (Table 3) with no measurable loss in its concentration or in the determined upper limit. Finally, the signal due to a known acetic acid concentration was the same in the presence and absence of OH. (OH reacted rapidly with the high concentration of acetone present). Thus, we believe that there was no significant loss of acetic acid on the flow tube wall or due to secondary reactions. We conservatively assign an upper limit to the acetic acid channel of <1%.

In summary, our results show that the yield of acetic acid (channel 1b) is very small (<0.01). The yield for acetonyl radical (channel 1a) is essentially unity at temperatures between 242 and 351 K.

3.3. Search for an OH−Acetone Adduct. If an OH−acetone adduct bound by more than ~10 kcal mol^{-1} is formed in reaction 1, its existence will manifest itself in measured temporal profiles of OH and the signal levels of OH.[21] Here, we derive an upper limit for the binding energy of an adduct using two methods: (a) from the observed temporal profiles of OH and (b) from the decrease of LIF signal upon the addition of varying amounts of acetone/acetone-d_6. To account for the decrease in LIF signal due to the removal of $OH(A^2\Sigma)^+$ by acetone, we also measured the rate coefficient, k_q, for this process.

The apparatus and the experimental technique used here are much the same as those used for measuring the rate coefficients for reactions 1 and 2; they are described in part 1.[1] The data acquisition methodology is similar to that used in previous studies.[22,23]

(a) We derive here an upper limit for the binding enthalpy of an OH−acetone complex based on the measured temporal profiles of OH in the presence of acetone. If adduct formation reaches equilibrium in tens or hundreds of microseconds, the OH temporal profile may be nonexponential. In the case of reaction 1, the temporal profiles were strictly exponential over at least 2 orders of magnitude of [OH] at all temperatures and time scales examined in our study (see Figure 5). The shortest delay time between the photolysis and probe lasers was 2 μs. Conservatively, we assume that if the adduct were formed, the relaxation time, τ, to reach equilibrium was less than 10 μs, i.e., 5 times longer than the shortest delay between the photolysis and the probe lasers. Assuming that the rate of decomposition

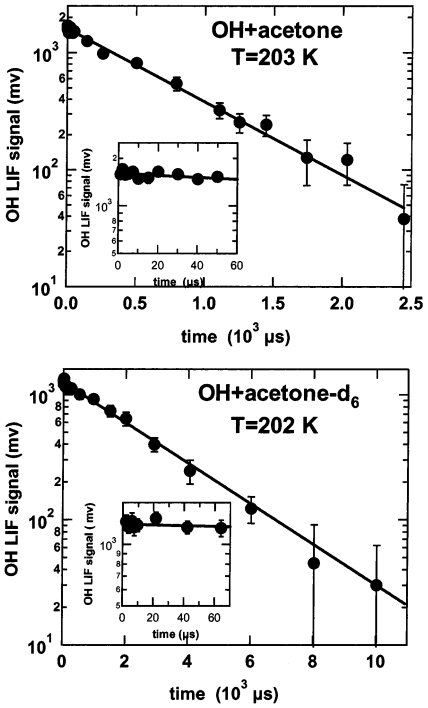

Figure 5. The temporal profiles of OH measured using PP-PLIF at 203 K in the presence of 4.7×10^{15} molecule cm^{-3} of acetone (upper panel) and 3.3×10^{15} molecule cm^{-3} of acetone-d_6 (lower panel). Exponential profiles in both cases show no evidence for equilibration of OH with the OH−acetone complex. The experiments were carried out in 100 Torr of He.

of the complex is much faster than its rate of formation under these conditions, τ is determined by the decomposition rate constant, k_r. Hence, k_r must be greater than $(10\ \mu s)^{-1}$, i.e., $>10^5$ s^{-1}. The ratio of the bimolecular rate constant (k_f) for the formation of the complex to its decomposition rate constant (k_r) is the equilibrium constant, K_c, i.e., $k_f/k_r = K_c$. For k_f, we have an upper limit of 2.67×10^{-11} cm^3 molecule^{-1} s^{-1}. This is the rate coefficient for the removal of OH ($v = 1$) by acetone determined in this work (see section 3.4), which should be similar to the rate coefficient for the formation of an OH−acetone complex in the limit of high pressure. Thus, we arrive

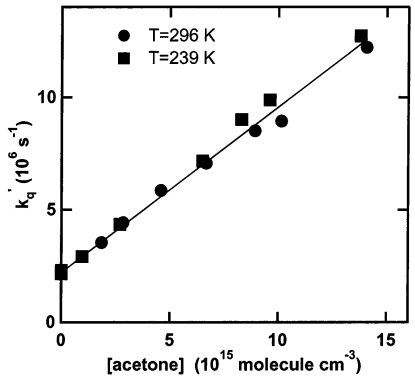

Figure 6. First order loss rate coefficient for the removal of electronically excited OH ($A^2\Sigma$) as a function of [acetone] at 296 K (filled circle) and 239 K (filled square). The slopes of the plots are k_q.

at an upper limit of 2.67×10^{-16} cm^3 molecule^{-1} for K_c at 203 K. This equilibrium constant leads to a value of K_P (referenced to standard states) of less than 9.7×10^3 at 203 K and a standard Gibbs free energy change, $\Delta_r G°$ ($=\Delta_r H° - T\Delta S°$), of greater than -3.7 kcal mol^{-1}. Assuming an entropy change ($\Delta S°$) for a weakly bound complex of -20 cal mol^{-1} ($\Delta S° = -22.8$ cal mol^{-1} for H-bonded complex with acetone at 200 K, from Aloisio and Francisco[10]), $\Delta_r H°$ is greater than -7.8 kcal mol^{-1} at 203 K.

(b) Another way to explore the possible formation of an adduct, even though the temporal profiles of OH were exponential, is to look for a decrease in the OH signals as the concentration of acetone is increased. Indeed, we noticed during our experiments that the OH signal decreased upon addition of acetone (acetone-d_6) to the reaction mixture. The decrease is due, at least in part, to the removal of electronically excited OH radicals ($A^2\Sigma^+$) by acetone. Both adduct formation and removal of OH ($A^2\Sigma^+$) occur together; thus, removal of OH ($A^2\Sigma^+$) by acetone could mask the adduct formation. We have measured the rate coefficient, k_q, for the removal of OH ($A^2\Sigma^+$) by acetone, using a method described elsewhere.[22] The pseudo-first-order rate coefficients for the removal of OH ($A^2\Sigma^+$), k_q', as a function of acetone concentration are plotted in Figure 6. The measured values of k_q for acetone are (in units of cm^3 molecule^{-1} s^{-1}): $(7.8 \pm 0.3) \times 10^{-10}$ at 296 K and $(7.4 \pm 0.1) \times 10^{-10}$ at 239 K. The rate coefficient for the removal of OH ($A^2\Sigma^+$) by acetone-d_6 at 296 K is $(7.6 \pm 0.1) \times 10^{-10}$ cm^3 molecule^{-1} s^{-1}. To our knowledge these rate coefficients have not been reported before. Our data indicates that, regardless of temperature or isotopic substitution, the rate coefficients for the removal of OH ($A^2\Sigma^+$) are essentially the same, and they are large. We measured the initial OH signals from fixed levels of OH in the presence of various concentrations of acetone at 239 and 221.5 K. The OH temporal profiles were strictly exponential. Analysis of these signals,[23] after accounting for the signal reduction due to quenching (using the rate coefficients reported above) resulted in $\Delta_r H^0 > -7.9$ kcal mol^{-1} at 239 K. This is similar to the value (> -7.8 kcal mol^{-1}) obtained from the measured OH temporal profiles discussed above. The above upper limits are consistent with the standard enthalpy of reaction for the formation of a hydrogen-bonded complex (complex A in Figure 7) of -7.2 kcal mol^{-1} at 200 K calculated by Aloisio and Francisco.[10] This small binding energy is consistent with our inability to observe the adduct. We can confidently conclude that if an adduct is formed, its binding enthalpy is less than 8 kcal mol^{-1} at 203 K.

It is also possible that the adduct, if it is formed and it lives long enough, could be scavenged by other reactants. Such scavenging by O_2 has been observed in many systems, e.g., in

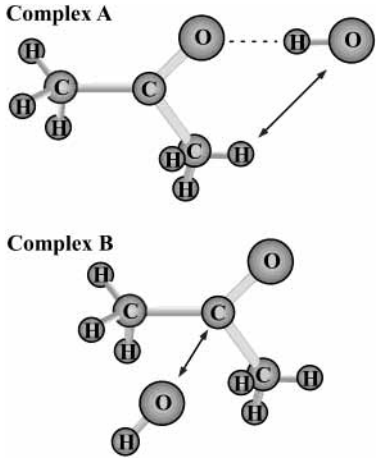

Figure 7. Two proposed structures for the adduct formed in the reaction of OH with acetone. Complex A is a hydrogen-bonded six-membered ring structure.[10] Complex B is α-hydroxyisopropoxy radical, $(CH_3)_2C(OH)O$, suggested by Wollenhaupt and Crowley.[2]

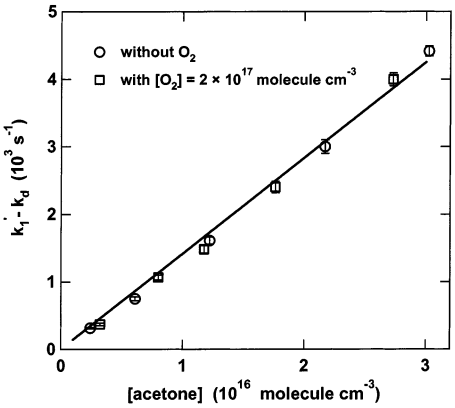

Figure 8. A plot of the pseudo-first-order rate coefficients for loss of OH (corrected for the loss in the absence of the reactant, k_d) vs acetone concentration in $\sim 2 \times 10^{17}$ molecule cm^{-3} of O_2 and 100 Torr N_2 (open square) and only 100 Torr of N_2 (open circle) at 213 K.

reactions of OH with aromatics,[24,25] CS_2,[17] and DMS.[17] Scavenging by O_2 is particularly important for atmospheric purposes, since the rate coefficient for acetone loss in the atmosphere could be larger if an adduct is formed and it reacts with O_2.

$$OH{\cdot}CH_3C(O)CH_3 + O_2 \rightarrow \text{products} \qquad (12)$$

If reaction 12 were fast, it would affect the OH decays in the presence of O_2. In all of our experiments, when oxygen was present (ca. 2×10^{17} molecule cm^{-3}) in the reactor, the OH decays were exponential. Several values of k_1 measured in the presence of oxygen do not differ substantially from those measured in He or N_2 in the absence of O_2 (e.g., see Figure 8). This suggests that either a stable complex is not formed and/or if formed it does not significantly react with O_2. Assuming conservatively that a 10% increase in the rate coefficient upon addition of O_2 would be observable, that such an increase would be linear in $[O_2]$, and that the upper limit for the binding enthalpy is -7.6 kcal mol^{-1} at 213 K, the value for k_{12} is $<3 \times 10^{-16}$ cm^3 molecule^{-1} s^{-1}.

^{18}OH Experiment. We also examined the possibility of a reaction where ^{18}OH exchanges with acetone to give ^{16}OH:

$$^{18}OH + CH_3C(^{16}O)CH_3 \rightarrow \text{products} \qquad (13a)$$

$$\rightarrow {}^{16}OH + CH_3C(^{18}O)CH_3 \qquad (13b)$$

TABLE 4: Reactions Used in the Numerical Simulation of ^{16}OH Temporal Profile in the Reaction of ^{18}OH with Acetone and their Rate Coefficients at 250 K

reaction	rate coefficient (cm^3 $molecule^{-1}$ s^{-1})	ref
$^{18}OH + CH_3C(^{16}O)CH_3 \rightarrow {}^{16}OH + CH_3C(^{18}O)CH_3$	variable (see the text)	
$^{18}OH + CH_3C(^{16}O)CH_3 \rightarrow$ products	variable (see the text)	
$^{16}OH + CH_3C(^{16}O)CH_3 \rightarrow$ products	1.43×10^{-13}	this work
$^{18}OH + O_3 \rightarrow H^{18}O^{16}O + O_2$	3.7×10^{-14} (same as $^{16}OH + O_3$)	17
$^{16}OH + O_3 \rightarrow HO_2 + O_2$	3.7×10^{-14}	17
$HO_2 + O_3 \rightarrow {}^{16}OH + 2O_2$	1.5×10^{-15}	17
$H^{18}O^{16}O + O_3 \rightarrow {}^{18}OH + 2O_2$	1.5×10^{-15}	17
$\rightarrow {}^{16}OH + O_2 + {}^{16}O^{18}O$	0	
$^{18}OH \rightarrow$ loss	50 s^{-1}	30
$^{16}OH \rightarrow$ loss	50 s^{-1}	30
$^{16}OH + H_2{}^{18}O \rightarrow {}^{18}OH + H_2{}^{16}O$	5.2×10^{-17}	31

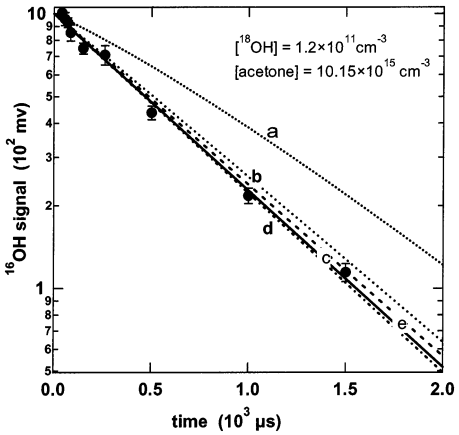

Figure 9. Simulated and measured temporal profiles of [^{16}OH] created by 248-nm photolysis of an $O_3/H_2{}^{18}O$/acetone mixture at 250 K. The [^{16}OH] profiles resulting from different fractions of reaction 13 that lead to exchange are shown: a, 50%; b, 10%; c, 5%; and d, 0%. The observed [^{16}OH] profile indicates that the rate coefficient for the exchange is $< 7 \times 10^{-15}$ cm^3 $molecule^{-1}$ s^{-1}. Curve e is a linear least-squares fit to data points. The mechanism used for the simulation is shown in Table 4.

Wollenhaupt et al. suggested that a α-hydroxyisopropoxy radical structure, shown as I below, formed when the oxygen

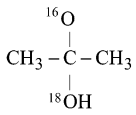

(I)

atom from hydroxyl radical attacks the carbonyl-C in acetone (complex B in Figure 7), could be the route for the formation of acetic acid.

If the reaction takes place by this mechanism, it is possible that the hydrogen atom could shift from the ^{18}O to the ^{16}O and the ^{16}OH radical may be released. At 250 K, we looked for the possible appearance of ^{16}OH in reaction 13b upon reaction of ^{18}OH with acetone using LIF as described in part 1.[1] The observed ^{16}OH temporal profile (^{16}OH and ^{18}OH were generated in equal amounts) was strictly exponential for at least two lifetimes (see Figure 9). The measured rate coefficient for ^{18}OH loss (see part 1) should show an increase over the rate coefficient for ^{16}OH if an exchange occurs. However, the rate coefficients for the loss of ^{18}OH and ^{16}OH were the same within the experimental uncertainty (see part 1). The ^{16}OH temporal profiles were computed[20] using the appropriate reactions and their rate coefficients (listed in Table 4) for various fractions of reaction 13 yielding ^{16}OH. Curve d in Figure 9 shows the profile expected for ^{16}OH when ^{18}OH did not exchange with $CH_3C(^{16}O)CH_3$. On the basis of such simulations, we place an upper limit of 7×10^{-15} cm^3 $molecule^{-1}$ s^{-1} (or 4% of the total reaction rate coefficient) for the rate coefficient for this exchange reaction.

3.4. Rate Coefficients for Removal of OH ($v = 1$) by Acetone and Acetone-d_6. The purpose of these experiments was to determine the rate coefficient for the formation of the possible OH−acetone complex. It has been argued that an estimate for the rate coefficient for the formation of a reactive complex of two species can be obtained by measuring the rate coefficient for removal of one species, excited with one quanta of vibration, by the other species.[26−28] Therefore, we measured the rate coefficients for the removal of OH ($v = 1$) by acetone and acetone-d_6

$$OH\ (v = 1) + CH_3C(O)CH_3 \rightarrow \text{loss of OH}\ (v = 1) \quad (14)$$

$$OH\ (v = 1) + CD_3C(O)CD_3 \rightarrow \text{loss of OH}\ (v = 1) \quad (15)$$

using a method described by McCabe et al.[28] OH ($v = 1$) was produced by the 248-nm laser photolysis of nitric acid. The temporal profile of OH ($v = 1$) was monitored via LIF by exciting the $Q_1(1)$ line of the $A^2\Sigma^+(v = 0) \leftarrow X^2\Pi(v = 1)$ band ($\lambda_{air} = 345.8516$ nm) and monitoring the fluorescence from the $A^2\Sigma^+(v = 0) \rightarrow X^2\Pi(v = 0)$ band at ~308 nm. The analysis of the temporal profiles of OH ($v = 1$) in the presence of various concentrations of acetone and acetone-d_6 yielded k_{14} and k_{15} values of $(2.67 \pm 0.15) \times 10^{-11}$ and $(3.45 \pm 0.24) \times 10^{-11}$ cm^3 $molecule^{-1}$ s^{-1}, respectively, at 295 K. k_{14} and k_{15} are upper limits for the rate coefficients for OH and acetone/acetone-d_6 complex formation. We have used this value to place an upper limit for $\Delta_r H°$ for the formation of an adduct, as described earlier. Also, the facts that reactions 14 and 15 are fast and the rate coefficients k_{14} and k_{15} are similar in magnitude support the hypothesis that OH and acetone indeed form a complex.

4. Discussion

4.1. Product Yields: Comparison with Previous Measurements. We have assigned an upper limit for the branching ratio for the channel in reaction 1 that leads to acetic acid, k_{1b}/k_1, of <1%. We have also shown that $CH_3C(O)CH_2$ is the primary (>85%) product of reaction 1. Wollenhaupt and Crowley[2] measured methyl radical formation resulting from reaction 1b using an indirect method. They converted methyl radical to CH_3O via reaction with NO_2 and measured the formation and decay of CH_3O radicals.

$$CH_3 + NO_2 \rightarrow CH_3O + NO \quad (16)$$

They extracted the branching ratio $\alpha = (k_{1b}/k_1)$ from the fit of the measured temporal profiles of CH_3O using a computer simulation of a fairly complex reaction mechanism. They determined α to be 0.5 and 0.3 at 297 and 233 K, respectively.

These results are surprising. One would expect that α would increase with decreasing temperature because channel 1b is an adduct-elimination pathway. The authors acknowledged this puzzling feature. Vasvári et al.[3] reported the yield of acetonyl radical (channel 1a) to be 50% relative to the reaction of F atom with acetone. They used a discharge flow tube equipped with resonance fluorescence detection of OH and laser-induced fluorescence of $CH_3C(O)CH_2$. They concluded, by subtraction, that the acetic acid yield is roughly 50%. Vandenberk et al.[5] recently reported an upper limit of ~5% for the acetic acid producing channel 1b based on experiments carried out in a discharge flow tube equipped with an electron impact mass spectrometer for direct detection of acetic acid. Tyndall et al.[4] studied reaction 1 in 1 atm of air at 296 and 251 K. They used in situ detection of the products by FTIR in a multipass cell. They did not observe any acetic acid production and reported an upper limit of <10% for the yield of acetic acid (channel 1b). They concluded that the reaction of OH with acetone proceeds predominantly (>90%) via H-atom abstraction.

The results of Vandenberk et al.,[5] Tyndall et al.,[4] and this work appear to contradict the findings of Vasvári et al.[3] and Wollenhaupt and Crowley.[2] Therefore, it is worthwhile to enquire if there are possible explanations for the observed differences.

Vasvári et al.[3] measured the yield of acetonyl radical to be ~50% at 298 K using DF/LIF in ~2 Torr of He carrier gas. They used the reaction of F atoms with H_2O to produce OH and the reaction of F atoms with acetone to produce $CH_3C(O)CH_2$. On the basis of the monitored signal of $CH_3C(O)CH_2$ from reaction 1 relative to that from the reaction of F atom with acetone, they calculated the yield of $CH_3C(O)CH_2$ from reaction 1. Two possible reasons why they may have measured a yield of $CH_3C(O)CH_2$ lower than that actually produced by reaction 1 in their experiments are that (a) the initial concentrations of F and OH were not the same and/or (b) the signal due to $CH_3C(O)CH_2$ from reaction 1 was underestimated relative to that from the reaction of F with acetone. In addition, OH production from the reaction of F with H_2O could be suppressed by O atoms, which are inevitably produced in a microwave discharge of F_2 (in a quartz or glass reactor). Thus, it is likely that $[OH]_0$ is less than $[F]_0$ in the experiments of Vasvári et al., contrary to their assumption. Vandenberk et al.[5] have discussed the possible secondary reactions in the study by Vasvári et al. by carrying out numerical modeling of the experimental conditions of Vasvári et al. They suggested that the measured acetonyl yield in Vasvari et al.'s system could be as much as 32% lower than $[OH]_0$, even if the yield of acetonyl radical from reaction 1 is unity. In addition, it is not clear how well Vasvári et al. accounted for the loss of $CH_3C(O)CH_2$. The temporal profile of $CH_3C(O)CH_2$ in their paper clearly shows a very rapid loss and that loss appears to be nonexponential. Therefore, Vasvári et al. could have underestimated the yield of $CH_3C(O)CH_2$. Because of these reasons, it appears that the yield of $CH_3C(O)CH_2$ of 0.5 reported by Vasvári et al. may not be compelling. Nielsen et al.[19] showed that the reaction of F with acetone proceeds via two channels; the major channel (92 ± 3%) gives $CH_3C(O)CH_2$ radicals and HF, while the minor channel (8 ± 1%) gives CH_3 radicals and $CH_3C(O)F$. If the yield of $CH_3C(O)CH_2$ in the F atom reaction is taken to be 0.92, the results of Vasvári et al. would be even lower. Very recently, Imrik et al.[29] (from the same group as Vasvári et al.) reported that the yield of $CH_3C(O)CH_2$ decreased from near unity at 353 K to 0.45 at 243 K. Discussion of these results awaits their publication.

Wollenhaupt and Crowley[2] reported detecting CH_3O, produced presumably from the reaction of CH_3 radicals with NO_2, and deduced the yield of CH_3 in reaction 1. They considered various possibilities, aside from reaction 1, that could have led to CH_3 production and concluded that CH_3 is a primary product of reaction 1. There are many secondary reactions in their system that could eventually lead to CH_3O.Vandenberk et al.[5] have discussed some of these reactions and the reasons for the large CH_3 yield measured by Wollenhaupt and Crowley.[2] It is possible that Wollenhaupt and Crowley detected a species other than CH_3O. Alternatively, subsequent reactions of $CH_3C(O)CH_2$ may also have contributed to the detected CH_3O. Last, if reaction 1c (see below) were to occur, it could also lead to CH_3O. However, as shown below, the branching ratio for channel 1c is small and cannot account for all the CH_3O detected by Wollenhaupt and Crowley. In any case, given the indirect nature of their experiments and the many secondary reactions that may lead to CH_3O, quantification of CH_3 yield in their study is difficult. Furthermore, given the small yield of CH_3O and the difficulties in detecting it, it does not appear prudent to use the time at which the CH_3O signal is maximized as a discriminator of various pathways for its production.

Tyndall et al.[4] carried out their study in air and it is not possible to rule out scavenging by O_2 of the adduct formed en route to acetic acid. High-pressure measurements of acetic acid yield in the absence of O_2 would be useful.

We have shown that the majority of the reaction proceeds via channel 1a, yielding $CH_3C(O)CH_2$ as one of the major products. We have also shown that a minor channel (1b) in reaction 1 is small and assigned an upper limit for the yield of this channel. Another possible exothermic channel of reaction 1 is 1c.

$$OH + CH_3C(O)CH_3 \rightarrow CH_3CO + CH_3OH \qquad \Delta_rH^0 = -8.0 \text{ kcal mol}^{-1} \quad (1c)$$

Because the yield of $CH_3C(O)CH_2$ is large, >85%, we conclude that the yield of other possible products via channel 1c is also small. Detection of CH_3OH in our system would have been useful; however, such measurements were not carried out.

4.2. Mechanism of OH + Acetone Reaction. Any mechanism of reaction 1 has to account for the following observations: (1) The yield of acetonyl radical is 96 ± 11% between 242 and 351 K in the pressure range 1−3 Torr. The yield of $CD_3C(O)CD_2$ in reaction 2 is also the same as the yield of $CH_3C(O)CH_2$ in reaction 1. (2) The yield for acetic acid, i.e., k_{1b}/k_1, is <1% between 237 and 353 K in the pressure range 1−3 Torr in He. Note that these yields are likely applicable at higher pressures, since k_1 does not change with pressure. (3) The Arrhenius plot of k_1 is curved (see part 1). Above ~240 K, k_1 increases with increasing temperature; below 240 K, k_1 reaches a constant value of $\sim 1.4 \times 10^{-13}$ cm^3 molecule^{-1} s^{-1}, independent of temperature between 199 and 240 K. A similar temperature trend (with a lower magnitude rate coefficient) has been observed for reaction 2. (4) The values of k_1 are independent of pressure (1−100 Torr of He or N_2). The value of k_1 measured at 250 K in 490 Torr of SF_6 is the same as that measured at lower pressures, i.e., down to 1 Torr of He, at that temperature. (5) There is a large primary kinetic isotope effect ($k_1 > k_2$) and a small secondary kinetic isotope effect (see part 1). (6) The rate coefficients k_{14} and k_{15}, for the removal of OH ($v = 1$) by acetone and acetone-d_6, are large and similar in magnitude. (7) ^{18}OH does not significantly exchange with acetone to generate ^{16}OH as a product. (8) The binding enthalpy

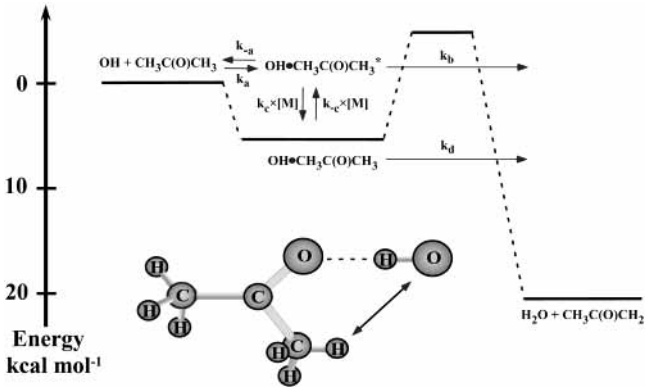

Figure 10. A representation of the mechanism for the reaction of OH with acetone, including the relative energetics of reactants and products.[5] The individual rate coefficients for various processes are also indicated.

of a possible $OH{\cdot}CH_3C(O)CH_3$ adduct is less than 8.0 kcal mol^{-1} at 203 K.

A mechanism for reaction 1 that is consistent with these observations is shown in Figure 10. This mechanism is very similar to that proposed for the reaction of OH with nitric acid, and the reader is referred to a previous paper from our group[8] about this reaction for a detailed discussion of the mechanism. The first step is the formation of an excited complex, $OH{\bullet}CH_3C(O)CH_3$*, via a barrierless addition of OH to $CH_3C(O)CH_3$. The excited complex may redissociate to the reactants, react to form products via collisional excitation over the barrier or tunneling, or be collisionally stabilized to form thermalized $OH{\bullet}CH_3C(O)CH_3$. The thermalized complex also decomposes to form products or may be reactivated to form $OH{\bullet}CH_3C(O)CH_3$*.

The doubly hydrogen-bonded six-membered ring complex shown as A in Figure 7 appears to be the plausible reactive complex in reaction 1. The structure of the complex is essentially identical to that proposed by previous investigators.[3,5,7,10] This complex is oriented to lead to a transition state for H-atom transfer from acetone to OH, which would lead to the observed products, $CH_3C(O)CH_2$ and H_2O. It is also consistent with the fact that acetic acid was not observed as a product (<1%) in this study and the lack of measurable exchange of ^{18}OH and ^{16}OH from reaction 13. Furthermore, recent ab initio calculations by several groups have predicted that such a complex will be stable with respect to the reactants and discussed the likelihood of this complex being the reactive complex in reaction 1.[3,5,7,10]

The temperature dependence of k_1 can be explained using the mechanism presented in Figure 10. If $OH{\bullet}CH_3C(O)CH_3$ and $OH{\bullet}CH_3C(O)CH_3$* are assumed to be in steady-state, the mechanism shown in Figure 10 leads to an analytical expression for k_1. Assuming that the measured rate coefficients represent the high-pressure limits for k_1, which is consistent with the pressure independence observed for this reaction, leads to the expression

$$k_1 = k_a\left(\frac{k_b + K_{eq}k_d}{k_{-a} + k_b + K_{eq}k_d}\right) \qquad \text{(II)}$$

The individual rate coefficients k_a, k_b, etc., are for the processes shown in Figure 10; K_{eq} is the equilibrium constant between the excited and stabilized complex (k_c/k_{-c}). Using the measured value of k_{14} at 295 K for k_a at all temperatures and the ab initio thermochemistry and vibrational frequencies calculated by Aloisio and Francisco,[10] k_{-a} and K_{eq} can be straightforwardly estimated[8] as a function of temperature. The remaining rate coefficients k_b and k_d were then fit as a function of temperature using the measured values of k_1. The estimated values of k_{-a} and K_{eq} and the fit values of k_b and k_d are shown in Table 5 at several temperatures, and the fit of k_1 as a function of temperature is shown in Figure 11.

TABLE 5: Rate Coefficients of the Individual Reactions in the Mechanism, Shown in Figure 10, Used to Simulate k_1[a]

T (K)	K_{eq}	k_{-a} (10^9 s^{-1})	k_b (10^7 s^{-1})	k_d (10^7 s^{-1})
400	0.2	29.3	40.1	110.0
340	0.5	10.0	8.1	8.1
300	1.2	3.9	2.4	0.95
240	8.4	0.5	0.25	0.015
220	20.1	0.2	0.098	0.0024
200	57.3	0.07	0.033	0.00029

[a] The simulated and experimental results are shown in Figure 11.

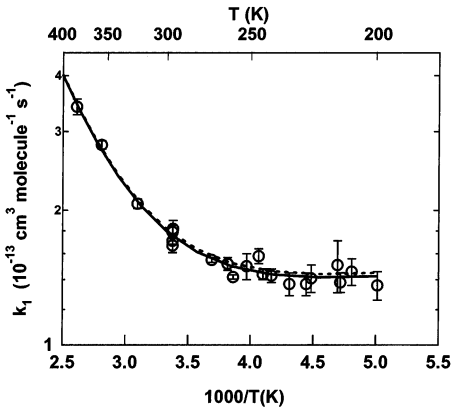

Figure 11. Comparison of the values of k_1 calculated using the mechanism shown in Figure 10 and the values of the rate coefficients listed in Table 5 (dashed line) with the measured values (open circles), in Arrhenius form. The solid curve is a fit to our experimental values.

The mechanism shown in Figure 10 is also consistent with the kinetic isotope effects we have reported, because of the strong influence of tunneling upon k_b and k_d.[8] It is the substantial difference between the values of k_b and k_d that leads to the large KIE. Despite the presence of collisional activation and deactivation in the mechanism, pressure dependence is not observed for k_1 under the conditions we have studied, because the complex stabilization energy is fairly low (~5 kcal mol^{-1}).[5]

Wollenhaupt and Crowley[2] postulated that reaction 1 proceeds through two channels: direct hydrogen atom abstraction leading to $CH_3C(O)CH_2 + H_2O$ (channel 1a) and addition of the OH radical to the acetone molecule to form an α-hydroxyisopropoxy radical (complex B in Figure 7) with its subsequent dissociation yielding acetic acid and methyl radical (channel 1b). We did not observe acetic acid production and only assign an upper limit to channel 1b of <1%. Theoretical calculations by Vandenberk et al.[5] suggested that the addition−elimination channel (1b) of reaction 1 should be negligible at atmospheric temperatures. Vasvári et al.[3] performed theoretical calculations of OH addition to the carbonyl-C through a four-center transition state to form α-hydroxyisopropoxy radical, which could eliminate CH_3 radical and form acetic acid. However, they found that such a mechanism would have a substantial activation barrier, in contrast to their measured 50% yield for $CH_3C(O)CH_2$. Recently, Yamada et al.[7] measured k_1 and k_2 at 740 Torr of He in the temperature range 298−832 K. They calculated k_1 and k_2 using variational transition state theory and concluded that the dominant pathway is channel 1a. They suggested that the reaction takes place via a hydrogen-bonded six-membered ring complex below 450 K and direct abstraction at high temperature. Recently, Henon et al.[6] presented an ab initio

calculation of the potential energy surface for reaction 1. They concluded that production of $CH_3C(O)OH$ is unlikely in this reaction, which is again contrary to the conclusions of Wollenhaupt and Crowley[2] and Vasvári et al.[3]

5. Atmospheric Implications

It has been established in this work that the yield of acetic acid in the reaction of OH with acetone is negligible (<1%). The major channel is the production of acetonyl radical with >85% yield. We note that a unit yield for $CH_3C(O)CH_2$ radical is consistent with our results.

The possible formation of an OH−acetone adduct followed by its reaction with O_2 (reaction 12) can also be a loss pathway for acetone in the atmosphere. On the basis of our measured upper limits for $\Delta_r H°$ for the formation of an OH−acetone adduct and k_{12} (assumed to be independent of temperature), the contribution of this process to the rate coefficient for the removal of acetone via reaction with OH will be less than 1% at 277 K and 370 Torr. At lower temperatures this pathway could contribute more to the loss of acetone. However, such temperatures are generally only present higher in the troposphere, where photolysis is the dominant loss process for acetone.

The absence of acetic acid suggests that acetone degradation will not lead to an organic acid that could produce new aerosol in the atmosphere. Further, the formation of acetic acid could have led to the loss of the acetone−OH reaction products from the atmosphere via precipitation/rain out of acetic acid and prevented formation of HO_x.

The formation of $CH_3C(O)CH_2$ in reaction 1 will lead to more HO_x production via the subsequent reactions of this radical.

Acknowledgment. This work was funded in part by NOAA's Climate and Global Change program and in part by Health of the Atmosphere program. We thank E. R. Lovejoy for discussions during this work. We also thank Rich McLaughlin for fabrication and assembly of parts of the apparatus. DCM thanks NSF for a Graduate Research fellowship. We thank K. Imrik and E. Henon for sharing their results that were presented at the 17th International Symposium on Gas Kinetics. We are grateful to a reviewer for pointing out that $CH_3C(O)$ (channel 1c) could lead to CH_3 radicals and subsequently to CH_3O in the experiments of Wollenhaupt and Crowley.

References and Notes

(1) Gierczak, T.; Gilles, M. K.; Bauerle, S.; Ravishankara, A. R. *J. Phys. Chem. A* **2003**, *107*, 5014.

(2) Wollenhaupt, M.; Crowley, J. N. *J. Phys. Chem. A* **2000**, *104*, 6429.

(3) Vasvári, G.; Szilágyi, I.; Bencsura, Á.; Dóbé, S.; Bérces, T.; Henon, E.; Canneaux, S.; Bohr, F. *Phys. Chem. Chem. Phys.* **2001**, *3*, 551.

(4) Tyndall, G. S.; Orlando, J. J.; Wallington, T. J.; Hurley, M. D.; Goto, M.; Kawasaki, M. *Phys. Chem. Chem. Phys.* **2002**, *4*, 2189.

(5) Vandenberk, S.; Vereecken, L.; Peeters, J. *Phys. Chem. Chem. Phys.* **2002**, *4*, 461.

(6) Henon, E.; Canneaux, S.; Bohr, F.; Dóbé, S. *Phys. Chem. Chem. Phys.* **2003**, *5*, 333.

(7) Yamada, T.; Taylor, P. H.; Goumri, A.; Marshall, P. *J. Phys. Chem. A* **2003**, *107* (in press).

(8) Brown, S. S.; Burkholder, J. B.; Talukdar, R. K.; Ravishankara, A. R. *J. Phys. Chem. A* **2001**, *105*, 1605.

(9) Gierczak, T.; Ravishankara, A. R. Kinetics of the reaction of hydroxyl radicals with acetone. 16th International Symposium on Gas Kinetics, 2000, University of Cambridge, Cambridge, UK.

(10) Aloisio, S.; Francisco, J. S. *J. Phys. Chem. A* **2000**, *104*, 3211.

(11) Gleason, J. F.; Sinha, A.; Howard, C. J. *J. Phys. Chem.* **1987**, *91*, 719

(12) Lovejoy, E. R.; Murrells, T. P.; Ravishankara, A. R.; Howard, C. J. *J. Phys. Chem.* **1990**, *94*, 2386.

(13) Lovejoy, E. R.; Ravishankara, A. R.; Howard, C. J. *Int. J. Chem. Kinet.* **1994**, *26*, 551.

(14) Han, J.; Heaven, M. C.; Manke, G. C., II *J. Phys. Chem. A* **2002**, *106*, 8417.

(15) Jaffe, S.; Clyne, A. A. *J. Chem. Soc., Faraday Trans. 2* **1981**, *77*, 531.

(16) Bedjanian, Y.; Le Bras, G.; Poulet, G. *J. Phys. Chem. A* **1999**, *103*, 7017

(17) DeMore, W. B.; Sander, S. P.; Golden, D. M.; Hampson, R. F.; Kurylo, M. J.; Howard, C. J.; Ravishankara, A. R.; Kolb, C. E.; Molina, M. J. *Chemical Kinetics and Photochemical Data for use in Stratospheric Modeling*; Jet Propulsion Laboratory, 1997, JPL Publication 97-4.

(18) Büttner, R.; Maurer, G. *Ber. Bunsen-Ges. Phys. Chem.* **1983**, *87*, 877.

(19) Nielsen, O. J.; Johnson, M. S.; Wallington, T. J.; Christensen, L. K.; Platz, J. *Int. J. Chem. Kinet.* **2002**, *34*, 283.

(20) Malleson, A. M.; Kellett, H. M.; Myhill, R. G.; Sweetenham, W. P. *Facsimile User Guide*; United Kingdom Atomic Energy Authority, HAREWELL, 1990.

(21) Murrells, T. P.; Lovejoy, E. R.; Ravishankara, A. R. *J. Phys. Chem.* **1990**, *94*, 2381.

(22) Vaghjiani, G. L.; Ravishankara, A. R. *J. Chem. Phys.* **1987**, *87*, 7050.

(23) Wahner, A.; Ravishankara, A. R. *J. Geophys. Res.* **1987**, *92*, 2189.

(24) Atkinson, R. *Chem. Rev.* **1985**, *85*, 69.

(25) Tully, F. P.; Ravishankara, A. R.; Thompson, R. L.; Nicovich, J. M.; Shah, R. C.; Kreutter, N. M.; Wine, P. H. *J. Phys. Chem.* **1981**, *85*, 2498.

(26) Smith, I. W. M. *J. Chem. Soc., Faraday Trans.* **1997**, *93*, 3741.

(27) Smith, I. W. M.; Ravishankara, A. R. *J. Phys. Chem. A* **2002**, *106*, 4798.

(28) McCabe, D. C.; Brown, S. S.; Gilles, M. K.; Talukdar, R. K.; Ravishankara, A. R.; Smith, I. W. M. *J. Phys. Chem. A* **2003**, (submitted).

(29) Imrik, K.; Vasvári, G.; Farkas, E.; Szilágyi, I.; Sarzynski, D.; Dóbé, S.; Bérces, T.; Márta, F. Kinetic and laser spectrometric study of the acetonyl radical. 17th International Symposium on Gas Kinetics, 2002, University of Essen, Essen, Germany.

(30) Vaghjiani, G. L.; Ravishankara, A. R.; Cohen, N. *J. Phys. Chem.* **1989**, *93*, 7833.

(31) Dubey, M. K.; Mohrschladt, R.; Donahue, N. M.; Anderson, J. G. *J. Phys. Chem. A* **1997**, *101*, 1494.